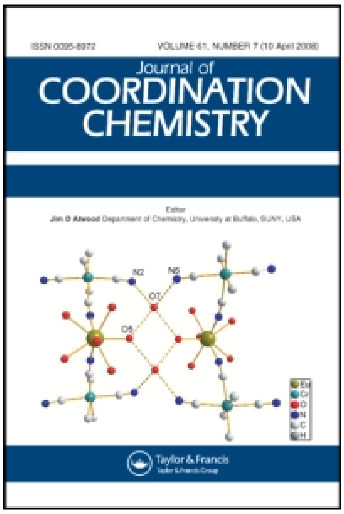

Journal of Coordination Chemistry
Publication details, including instructions for authors and subscription information:
http://www.informaworld.com/smpp/title~content=t713455674

Hydrothermal syntheses and characterizations of two new hydrogen bond-supported supramolecular compounds based on polyoxometalates

Shu-Yun Shi[a,b]; Jia-Ning Xu[a]; Wen-Ying MA[c]; Xiao-Bing Cui[a]; Yan Wang[a]; Guo-Wu Wang[a]; Ji-Qing Xu[a]
[a] Department of Chemistry, College of Chemistry and State Key Laboratory of Inorganic Synthesis and Preparative Chemistry, Jilin University, Changchun, China [b] Department of Environmental Engineering, Jilin Normal University, Siping, China [c] Department of Applied Chemistry and Pharmacy, Zhuhai College, Jilin University, Zhuhai, China

First published on: 22 September 2010

To cite this Article Shi, Shu-Yun , Xu, Jia-Ning , MA, Wen-Ying , Cui, Xiao-Bing , Wang, Yan , Wang, Guo-Wu and Xu, Ji-Qing(2009) 'Hydrothermal syntheses and characterizations of two new hydrogen bond-supported supramolecular compounds based on polyoxometalates', Journal of Coordination Chemistry, 62: 24, 3885 — 3894, First published on: 22 September 2010 (iFirst)

To link to this Article: DOI: 10.1080/00958970903207369

URL: http://dx.doi.org/10.1080/00958970903207369

Journal of Coordination Chemistry
Vol. 62, No. 24, 20 December 2009, 3885–3894

Hydrothermal syntheses and characterizations of two new hydrogen bond-supported supramolecular compounds based on polyoxometalates

SHU-YUN SHI†‡, JIA-NING XU†, WEN-YING MA§, XIAO-BING CUI*†,
YAN WANG†, GUO-WU WANG† and JI-QING XU*†

†Department of Chemistry, College of Chemistry and State Key
Laboratory of Inorganic Synthesis and Preparative Chemistry,
Jilin University, Changchun 130023, China
‡Department of Environmental Engineering, Jilin Normal University,
Siping 136000, China
§Department of Applied Chemistry and Pharmacy, Zhuhai College,
Jilin University, Zhuhai 519000, China

(*Received 8 April 2009; in final form 8 June 2009*)

Two new polyoxometalates $[HN(C_2H_5)_3]_3[PMo_{12}O_{40}]$ (**1**) and $[NH_2(C_2H_4NH_3)_2]_2[Mo_5P_2O_{23}]$ (**2**) have been hydrothermally synthesized and characterized by IR, UV-Vis, XPS spectra, TG analyses, and single crystal X-ray diffraction. Crystal data for **1**: monoclinic, space group $C2/c$, $a = 24.651(5)$ Å, $b = 10.822(2)$ Å, $c = 22.413(5)$ Å, $\beta = 120.37(3)^\circ$, and $V = 5158.7(18)$ Å^3; for **2**: triclinic, space group *P-1*, $a = 9.821(2)$ Å, $b = 9.948(2)$ Å, $c = 14.687(3)$ Å, $\alpha = 95.490(3)^\circ$, $\beta = 98.870(3)^\circ$, $\gamma = 95.710(3)^\circ$, and $V = 1401.7(5)$ Å^3. The crystal structure analyses reveal complex hydrogen bonds in both **1** and **2** in 3-D supramolecular arrays constructed from different polyoxoanions and organic ligands.

Keywords: Crystal structure; Hydrothermal synthesis; Hydrogen bond; Supramolecular framework

1. Introduction

Growth in supramolecular chemistry has been driven by increased synthetic and characterization methods for complex structures [1–3]. Directed assembly of supramolecular arrays from discrete molecular building blocks has applications in catalysis, molecular electronics, sensor design, and optics [4–9]. In the construction of supramolecular materials, discrete molecular building blocks generally extend to high-dimensional supramolecular arrays through hydrogen-bonding, $\pi \cdots \pi$ stacking, and weak van der Waals interactions; hydrogen-bonding is the most familiar organizing force in supramolecular assemblies by virtue of its unique strength and directionality for the control of short-range packing [10].

The spherical surface of polyoxometalates (POMs) gives an opportunity for forming hydrogen bonds with organic or inorganic moieties. Extensive efforts have been made

---

*Corresponding authors. Email: cuixb@mail.jlu.edu.cn; xjq@mail.jlu.edu.cn

Journal of Coordination Chemistry
ISSN 0095-8972 print/ISSN 1029-0389 online © 2009 Taylor & Francis
DOI: 10.1080/00958970903207369

to design and assemble such supramolecular architectures and a few high-dimensional supramolecular architectures have been synthesized [11–13]. Our group has several supramolecular architectures based on $\{V_{18}O_{42}\}$, $\{As_6V_{15}\}$, $\{AsW_{12}O_{40}\}$, $\{V_{15}O_{36}\}$, and $\{V_{16}O_{38}\}$ [12, 13].

A prominent subclass of POMs is the family of polyoxomolybdates which present a wide range of intriguing topologies and structures. However, the supramolecular compounds based on these POMs have been incompletely explored [14, 15]. Here, we begin our research by using the polyoxomolybdates as structural building blocks to prepare hydrogen-bonded supramolecular compounds with two new polyoxomolybdate-based supramolecular compounds, $[HN(C_2H_5)_3]_3[PMo_{12}O_{40}]$ (**1**) and $[NH_2(C_2H_4NH_3)_2]_2[Mo_5P_2O_{23}]$ (**2**). This article deals with the syntheses, structures, and characterizations of **1** and **2**. The crystal structure analyses reveal complex hydrogen bonds between organic moieties and the POMs.

2. Experimental

2.1. *Materials and methods*

All chemicals used were of reagent grade without purification. C, H, and N elemental analyses were carried out on a Perkin-Elmer 2400 CHN elemental analyzer. The elemental analyses of P and Mo were performed on a Perkin-Elmer Optima 3300DV spectrophotometer. Infrared spectra were recorded as KBr pellets on a Perkin-Elmer SPECTRUM ONE FTIR spectrophotometer. UV-Vis spectra were measured on a Shimadzu UV-3100 spectrophotometer. XPS analysis was performed on a VG ESCALAB MK II spectrometer with an Mg-Kα (1253.6 eV) achromatic X-ray source. The thermogravimetric (TG) curves were performed on a Perkin-Elmer TGA-7000 thermogravimetric analyzer in flowing air with a temperature ramp rate of $10^\circ C\,min^{-1}$.

2.2. *Synthesis*

2.2.1. Synthesis of $[HN(C_2H_5)_3]_3[PMo_{12}O_{40}]$ (1). A mixture of $(NH_4)_6Mo_7O_{24}\cdot 4H_2O$ (0.5 mmol), H_3PO_4 (0.1 mmol), Sb_2O_3 (0.25 mmol), $AgNO_3\cdot H_2O$ (0.5 mmol), triethylamine (TEA) (0.5 mmol), and H_2O (12 mL, 666 mmol) was stirred for 60 min, the pH was adjusted to 5 by addition of 1 M HCl and the suspension was then transferred to an 18 mL Teflon-lined autoclave and heated under autogenous pressure at 160°C for 3 days. The autoclave was then cooled to room temperature. Very pale block crystals were obtained, washed with distilled water and air-dried. Yield: 71% (based on Mo). Anal. Calcd for $C_{18}H_{48}Mo_{12}N_3O_{40}P$: C, 10.16; H, 2.27; N, 1.97; P, 1.45; Mo, 54.08%. Found: C, 10.35; H, 2.01; N, 2.07; P, 1.32; Mo, 54.11%.

2.2.2. Synthesis of $[NH_2(C_2H_4NH_2)_2][Mo_5P_2O_{23}]$ (2). A mixture of $(NH_4)_6Mo_7O_{24}\cdot 4H_2O$ (0.5 mmol), H_3PO_4 (0.1 mmol), Sb_2O_3 (0.25 mmol), $CuAc_2\cdot H_2O$ (0.5 mmol), 4-4′bipy · $2H_2O$ (0.5 mmol), piperazine (0.5 mmol), and H_2O (12 mL, 666 mmol) was stirred for 60 min and after adjustment of the pH to 3–4 by addition of 1 M HCl, the suspension was transferred to an 18 mL Teflon-lined autoclave and

Table 1. Crystal data and structure refinement parameters for **1** and **2**.

Compound	**1**	**2**
Empirical formula	$C_{18}H_{48}Mo_{12}N_3O_{40}P$	$C_8H_{32}Mo_5N_6O_{23}P_2$
Formula weight	2128.84	1122.04
Crystal system	Monoclinic	Triclinic
Space group	*C*2/*c*	*P-1*
Unit cell dimensions (Å, °)		
a	24.651(5)	9.821(2)
b	10.822(2)	9.948(2)
c	22.413(5)	14.687(3)
α		95.490(3)
β	120.37(3)	98.870(3)
γ		95.710(3)
Volume (Å^3), *Z*	5158.7(18), 4	1401.7(5), 2
Calculated density (mg m^{-3})	1.347	2.571
Absorption coefficient (mm^{-1})	1.473	2.338
F(000)	1959	1050
θ range for data collection (°)	2.11–26.10	2.34–26.10
Completeness to θ (%)	99.9	98.6
R_{int}	0.0348	0.0185
Goodness-of-fit on F^2	1.063	1.061
Final *R* indices [$I > 2\sigma(I)$]	$R_1 = 0.0430$, $wR_2 = 0.1089$	$R_1 = 0.0271$, $wR_2 = 0.0752$

$R_1 = \sum ||F_o| - |F_c|| / \sum |F_o|$; $wR_2 = \left[\sum w(F_o^2 - F_c^2)_2 / \sum w(F_o^2)^2\right]^{1/2}$.

heated under autogenous pressure at 160°C for 3 days. The autoclave was then cooled to room temperature. Gray crystals were obtained, washed with distilled water and air-dried. Yield: 85% (based on Mo). Anal. Calcd for $C_8H_{32}Mo_5N_6O_{23}P_2$: C, 8.56; H, 2.87; N, 7.49; P, 5.52; Mo, 42.75%. Found: C, 8.75; H, 2.49; N, 7.64; P, 5.71; Mo, 42.64%.

2.3. *X-ray crystallography*

The reflection intensity data for **1** and **2** were collected on a Rigaku R-AXIS RAPID IP diffractometer with graphite monochromated Mo-Kα ($\lambda = 0.71073$ Å) radiation at 293 K. Neither of the crystals showed evidence of crystal decay during the data collections. Both structures were solved by direct methods and refined using full-matrix least-squares on F^2 using SHELXTL-97 crystallographic software package. For **1**, all atoms were refined anisotropically except C and N; no H atoms were added. It should be noted that both N(2) and C(7) are disordered over two positions with occupancy factors of 0.5, while C(8) is located at a special position. For **2**, all the atoms were refined anisotropically and hydrogens were fixed at their ideal positions. A summary of the crystallographic data and structural refinements for **1** and **2** are given in table 1. Selected bond lengths are listed in table S1.

3. Results and discussion

3.1. *Synthesis*

The supramolecular compounds of this study were prepared by hydrothermal methods. Generally, many factors affect the products in hydrothermal reactions, such as initial reactants, stoichiometry, filling volume, pH, temperature, reaction time, etc. The pH is crucial for formation of **1** and **2**. Only when the pH value was 5, **1** was formed, and only when the pH was 3–4 **2** was formed. Sb_2O_3, $AgNO_3 \cdot H_2O$, and $CuAc_2 \cdot H_2O$ were absolutely important for the formations of **1** and **2**, though Sb, Ag, or Cu were not incorporated into the final products. If we did not add them (other reaction conditions left unchanged), only undetermined powders were obtained. Reactions for synthesis of **1** and **2** were not sensitive to temperature in the range 160–180°C and 3–5 days, respectively.

Diethylene triamine (DETA) in **2** was *in situ* synthesized, though the mechanism for formation of DETA is elusive. To date, more than 10 types of *in situ* species formation reactions have been reported, including carbon–carbon bond formation [16], hydroxylation [17], ether bond formation [18], decarboxylation [19], tetrazole and triazole formation [20], alkylation [21], hydrolysis [22], transformation between inorganic and organic sulfur [23], acylation [24], and isomerization [25]. Hydrothermal *in situ* species synthesis has been noted extensively due to its effectiveness, simplicity, and environmental friendliness [26] and is a very useful pathway to obtain organic species, which is difficult to obtain by routine synthetic methods [20–24].

We tried to synthesize **2** by using DETA directly with $(NH_4)_6Mo_7O_{24} \cdot 4H_2O$, H_3PO_4, and H_2O under the same hydrothermal conditions but were not successful.

3.2. *Crystal structure of 1*

Crystal structure analysis reveals that **1** consists of $[PMo_{12}O_{40}]^{3-}$ and protonated TEA. As shown in figure 1, $[PMo_{12}O_{40}]^{3-}$ which exhibits a typical pseudo-Keggin core [27] is based on a central PO_4^{3-} tetrahedron surrounded by 12 $\{MoO_6\}$ octahedra arranged in four groups of internally edge-sharing tri-octahedra Mo_3O_{13}. These Mo_3O_{13} are linked by sharing corners to each other and to the central PO_4^{3-}. In the anion, each oxygen of the central PO_4^{3-} tetrahedron is disordered over two positions with occupation factors of 0.5, forming an almost regular cubic motif. The P–O distances vary from 1.511(8) to 1.539(8) Å and the oxygens can be divided into three groups: O_t (terminal O atoms), O_b (bridging O atoms), and O_c (O atoms of the center). The Mo–O_t distances are 1.646(5)–1.667(5) Å, Mo–O_b distances are 1.805(6)–2.014(6) Å, and Mo–O_c distances are

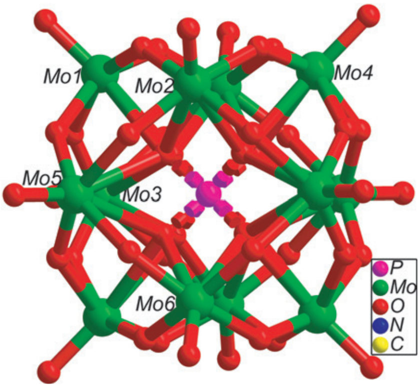

Figure 1. Ball-and-stick representation of $[PMo_{12}O_{40}]^{3-}$ in **1**.

2.448(8)–2.497(8) Å, respectively (table S1). These results show that the $\{MoO_6\}$ octahedra are distorted, resulting in decrease of symmetry of $[PMo_{12}O_{40}]^{3-}$ [28]. The bond lengths and angles of **1** are comparable to phosphomolybdates reported [29–31].

The bond valence sum (BVS) values [32] for the six crystallographically independent molybdenums Mo_1–Mo_6 of **1** are 6.15, 6.15, 6.24, 6.16, 6.19, and 6.13, respectively, indicating the molybdenums are +6 oxidation state, consistent with the anions $[X^{n+}Mo_{12}O_{40}]^{(8-n)}$ (X^{n+} represents a variety of heterocations with oxidation states +4 or +5) [33].

As illustrated in figure 2, the $[PMo_{12}O_{40}]^{3-}$ anion is linked with the adjacent one through four O $\cdots$ O interactions propagating along the *b* axis to form a 1-D chain structure; the O $\cdots$ O interactions have O $\cdots$ O distances of 3.1756(6) Å for O4 $\cdots$ O18 ($2-x$, $1-y$, $1-z$) (and its symmetry equivalent) and 3.1814(6) Å for O9 $\cdots$ O18 ($2-x$, $1-y$, $1-z$) (and its symmetry equivalent). The chain is further connected with the adjacent one into a 2-D infinite layer structure via O $\cdots$ O interactions with distances of 3.0039(6) Å for O7 $\cdots$ O16 ($x, -y, -0.5+z$) (and its symmetry equivalents). These distances between oxygen atoms are in the range of distances for hydrogen bonds.

The structure of **1** also contains complex C–H $\cdots$ O hydrogen-bonding interactions. The TEA cation containing N1 (TEA **1**) bridges two adjacent POMs through hydrogen-bonding interactions of C2–H $\cdots$ O11 ($-0.5+x, 1.5-y, 0.5+z$), C3–H $\cdots$ O9 ($1.5-x$, $0.5+y, 1.5-z$), and C4–H $\cdots$ O2 ($-0.5+x, 1.5-y, 0.5+z$) with distances of 3.353(6) Å, 3.393(6) Å, and 3.323(6) Å, respectively (figure S1(a)), while the TEA cation containing N2 (TEA **2**) connects three neighboring POMs via hydrogen-bonding interactions of C7–H $\cdots$ O13 ($x, 1+y, z$) (and its symmetry equivalent), C9–H $\cdots$ O4 ($-0.5+x, 0.5+y, z$), C10–H $\cdots$ O4 ($-0.5+x, 0.5+y, z$), and C10–H $\cdots$ O10 ($-0.5+x$, $0.5+y, z$) with distances of 3.330(6) Å, 3.148(6) Å, 3.288(6) Å, and 3.335(6) Å, respectively (figure S1(b)). Each POM links four TEA **1** and four TEA **2** cations through C–H $\cdots$ O hydrogen-bonding interactions. TEA **1** and the TEA **2** cations are alternatively disposed around the central POM (figure S1(c)). Thus, hydrogen-bonding interactions between oxygens from the POMs and carbons from different TEA cations connect the POMs and the TEA cations into an interesting 3-D supramolecular network.

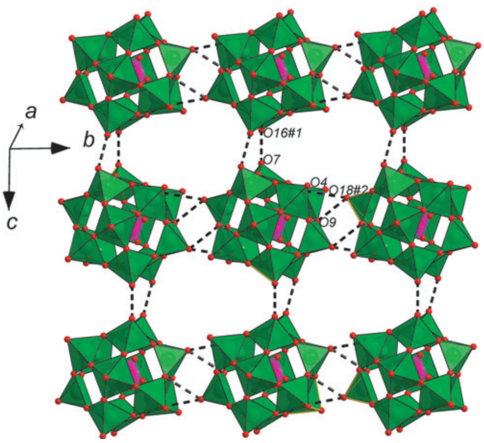

Figure 2. View of the 2-D layer structure of **1** constructed from O $\cdots$ O interactions among the POMs. The TEA ligands have been omitted for clarity.

The topological representation of **1** constructed from the POMs and TEA through C–H $\cdots$ O interactions is depicted in figure 3. Each POM as a node connects four adjacent TEA **1** and four adjacent TEA **2** cations, alternately; TEA **1** links two adjacent POMs, while TEA **2** joins three adjacent POMs. In this way, the POMs and the TEA groups assemble into a 3-D supramolecular network through complex C–H $\cdots$ O hydrogen-bonding interactions.

In summary, there exist two different interactions in **1**, O $\cdots$ O interactions and the C–H $\cdots$ O hydrogen-bonding interactions. These synergistic interactions increase the stability of the structure of **1**.

3.3. *Crystal structure of 2*

Compound **2** is composed of $[Mo_5P_2O_{23}]^{6-}$ similar to reported compounds [34] and protonated DETA (figure 4). The $[Mo_5P_2O_{23}]^{6-}$ anion can be viewed as two PO_4^{3-}

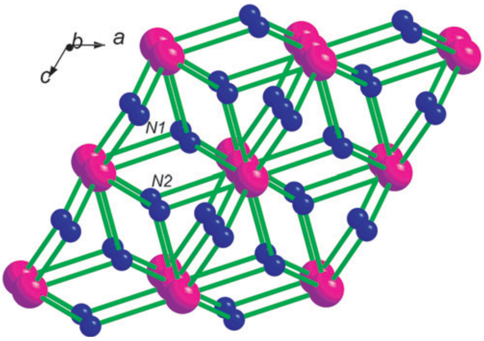

Figure 3. Topological representation of the 3-D supramolecular network structure of **1** formed through the C–H $\cdots$ O hydrogen-bonding interactions between $[PMo_{12}O_{40}]^{3-}$ and TEA. The big circles represent $[PMo_{12}O_{40}]^{3-}$, the small circles represent TEA cation, and the lines represent hydrogen bonds.

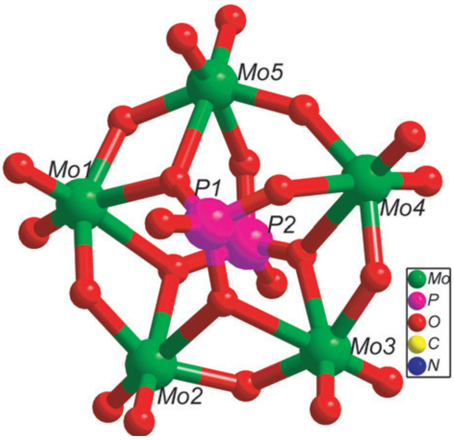

Figure 4. Ball-and-stick representation of $[Mo_5P_2O_{23}]^{6-}$ in **2**.

tetrahedra capping either side of an irregular ring of five $\{MoO_6\}$ octahedra linked by one corner-shared and four edge-shared contacts. The oxygens which connect molybdenums can be grouped into terminal oxygens O_t, bridging oxygens O_b, and central oxygens O_c. Thus the Mo–O bond lengths can be grouped as Mo–O_t 1.700(3)–1.726(3) Å, Mo–O_b 1.896(3)–1.964(3) Å, and Mo-O_c 2.205(3)–2.388(3) Å. Each phosphorus has one terminal oxygen, one double bridging oxygen, and two triple bridging oxygens. The P–O_t bond lengths are in the range 1.524(3)–1.553(3) Å, while the P–O_b bond lengths range from 1.517(3) to 1.558(3) Å (table S1).

The BVS values [32] for the five crystallographically independent molybdenums Mo_1–Mo_5 of **2** are 5.87, 5.93, 5.91, 5.89, and 5.91, and the BVS values for the two crystallographically independent phosphorus atoms are 5.02 and 4.99, respectively.

A striking feature of **2** is that it exhibits an unusual 3-D supramolecular network structure constructed from the DETA cations and the $[Mo_5P_2O_{23}]^{6-}$ anions through N–H···O hydrogen bonds. There exist two kinds of linking modes between DETA and $[Mo_5P_2O_{23}]^{6-}$. One is that DETA containing N1, N2, and N3 (DETA **1**) joins four adjacent anions through hydrogen-bonding interactions of N1–H···O14, N1–H···O23 $(1-x, 1-y, 1-z)$, N2–H···O13 $(1-x, 1-y, 1-z)$, N2–H···O23, N3–H···O11 $(2-x, 2-y, 1-z)$, N3–H···O15, N3–H···O17 $(2-x, 1-y, 1z)$, and N3–H···O23 with distances of 2.887(6) Å, 2.916(6) Å, 2.825(6) Å, 2.627(6) Å, 2.862(6) Å, 2.760(6) Å, 2.813(6) Å, and 2.999(6) Å (figure S3(a)). The other linking mode is that DETA containing N4, N5, and N6 (DETA **2**) links three adjacent POMs via hydrogen-bonding interactions of N4–H···O7 $(x, 1+y, z)$, N4–H···O11, N5–H···O10, N6–H···O1 $(2-x, 1-y, 2-z)$, N6–H···O7 $(2-x, 1-y, 2-z)$, N6–H···O8, and N6–H···O10 with distances of 2.868(6) Å, 2.964(6) Å, 2.571(6) Å, 2.855(6) Å, 2.934(6) Å, 2.780(6) Å, and 2.878(6) Å, respectively (figure S3(b)). Alternatively, each POM links four DETA **1** and three DETA **2** cations through N–H···O hydrogen-bonding interactions (figure S1(c)). These synergistic interactions increase the stability of **2**. $[Mo_5P_2O_{23}]^{6-}$ and the different DETA cations are linked by complex hydrogen bonds (N–H···O) (table 2) to give the complex 3-D supramolecular network structure.

Table 2. Hydrogen bond parameters for **1** and **2**.

	D–H···A (Å)		D–H···A (Å)
Compound **1**			
C2–H···O11(#1)	3.353(6)	C9–H···O4(#4)	3.148(6)
C3–H···O9(#2)	3.393(6)	C10–H···O4(#4)	3.288(6)
C4–H···O2(#1)	3.323(6)	C10–H···O10(#4)	3.335(6)
C7–H···O13(#3)	3.330(6)		
Compound **2**			
N1–H···O14	2.887(6)	N4–H···O7(#4)	2.868(6)
N1–H···O23(#1)	2.916(6)	N4–H···O11	2.964(6)
N2–H···O13(#1)	2.825(6)	N5–H···O10	2.571(6)
N2–H···O23	2.627(6)	N6–H···O1(#5)	2.855(6)
N3–H···O11(#2)	2.862(6)	N6–H···O7(#5)	2.934(6)
N3–H···O15	2.760(6)	N6–H···O8	2.780(6)
N3–H···O17(#3)	2.813(6)	N6–H···O10	2.878(6)
N3–H···O23	2.999(6)		

Symmetric components for **1** – #1: $-0.5+x$, $1.5-y$, $0.5+z$; #2: $1.5-x$, $0.5+y$, $1.5-z$; #3: x, $1+y, z$; #4: $-0.5+x$, $0.5+y$, z.
Symmetric components for **2** – #1: $1-x$, $1-y$, $1-z$; #2: $2-x$, $2-y$, $1-z$; #3: $2-x$, $1-y$, $1-z$; #4: x, $1+y$, z; #5: $2-x$, $1-y$, $2-z$.

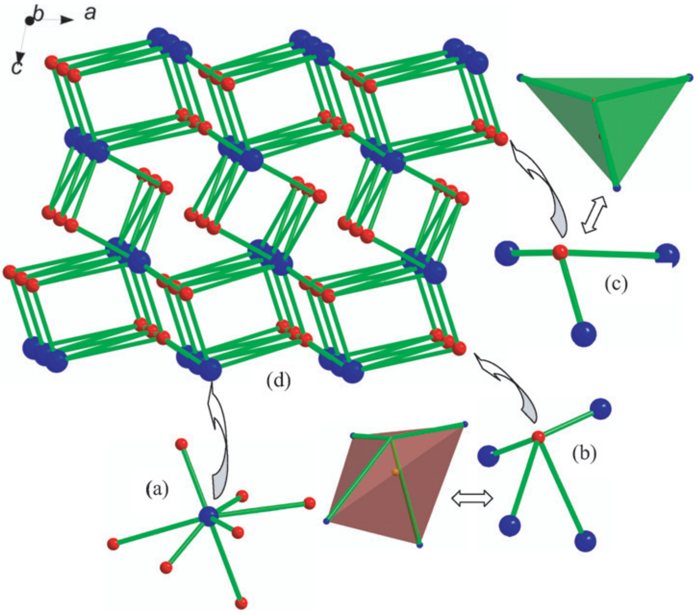

Figure 5. (a) $[Mo_5P_2O_{23}]^{6-}$ as a 7-connected node. (b) DETA **1** cation interacts with four clusters displaying distorted tetrahedral configuration. (c) DETA **2** bridges three neighboring $[Mo_5P_2O_{23}]^{6-}$ clusters generating distorted pyramidal coordination. (d) Topological representation of the 3-D network of **2** formed through N–H···O hydrogen bonds between $[Mo_5P_2O_{23}]^{6-}$ and DETA cations. The big circles represent $[Mo_5P_2O_{23}]^{6-}$, the small circles represent DETA cation, and the lines represent hydrogen bonds.

A topology view of **2** is shown in figure 5. The $[Mo_5P_2O_{23}]^{6-}$ acts as a seven-connected node, interacting with seven adjacent DETA cations (figure 5a), while DETA **1** interacts with four adjacent $[Mo_5P_2O_{23}]^{6-}$ anions disposed tetrahedrally around DETA **1**, exhibiting a distorted tetrahedral motif (figure 5b). The DETA **2** bridges three neighboring $[Mo_5P_2O_{23}]^{6-}$ anions generating a distorted pyramidal motif, in which DETA **2** is located at the apical site and the three anions are located at the bottom (figure 5c). In summary, each DETA cation is a three-connected node or a four-connected node further connecting three or four neighboring $[Mo_5P_2O_{23}]^{6-}$ to generate a 3-D structure (figure 5d).

3.4. *IR, UV-Vis, and XPS spectra*

The IR spectrum (figure S3) for **1** shows an intense band at 1060 cm^{-1} ascribed to ν(P–O) and bands at 961 cm^{-1}, 879 cm^{-1}, and 803 cm^{-1} ascribed to $\nu(Mo–O_t)$, $\nu(Mo–O_b–Mo)$, and $\nu(Mo–O_c–Mo)$, respectively [35]. A series of bands in the region 1629–1114 cm^{-1} are attributed to vibrations of TEA. The IR spectrum (figure S3) for **2** exhibits a band at 1055 cm^{-1} ascribed to ν(P–O) and bands at 915 and 817 cm^{-1} for stretching vibrations of $Mo–O_t$ and Mo–O–Mo, respectively. Bands at 1599–1145 cm^{-1} can be attributed to vibrations of DETA.

The UV-Vis spectra for **1** and **2** are presented in figure S4. The UV-Vis spectrum for **1** exhibits two broad absorptions at 232 and 318 nm assigned to O→Mo charge transfer in $[PMo_{12}O_{40}]^{3-}$ [36]. The UV-Vis spectrum for **2** exhibits two overlapped bands at 229 and 276 nm attributed to O→Mo charge transfer in $[Mo_5P_2O_{23}]^{6-}$. The XPS spectra for **1** and **2** are very similar (figure S5) with peaks at 232.9 and 236 eV for **1** and 232.5 and 235.6 eV for **2**, from molybdenum (Mo $3d_{5/2}$ and Mo $3d_{3/2}$) with +6 oxidation state for both compounds.

3.5. *Thermogravimetric analysis*

The TG analyses for **1** and **2** are shown in figure S6. The TGA curve for **1** is similar to that of **2** showing weight losses that cannot be completely divided into individual stages. Total weight losses for **1** and **2** were in accord with the calculated values. Compound **1** is stable from room temperature to 271°C, in the range 271–454°C, the total weight loss is 15.24% (calculated value: 14.40%), corresponding to the release of TEA (figure S6-1). For **2**, from 155 to 483°C, the weight loss is 18.69% (calculated value: 18.93%), corresponding to the loss of DETA (figure S6-2).

4. Conclusions

Two compounds based on different polyoxoanion clusters and organic moieties have been synthesized and structurally characterized. Syntheses of **1** and **2** provide low-dimensional inorganic building blocks with various organic moieties extending to high-dimensional supramolecular networks through hydrogen-bonding interactions. Supramolecular interactions among the organic molecules and inorganic polyanions play significant roles in stabilization of the overall high-dimensional supramolecular network. Research is underway to reveal the synthetic rules and explore the properties of POM-based supramolecular materials.

Supplementary material

CCDC reference numbers: 720533 for **1** and 720534 for **2**.

Acknowledgment

This work was supported by the National Natural Science Foundation of China (Grant Nos 20571032 and 20333070).

References

[1] J.M. Lehn. *Supramolecular Chemistry*, VCH, New York (1995).
[2] F. Vögtle. *Supramolecular Chemistry*, Wiley, Chichester (1991).
[3] J.M. Lehn. *Comprehensive Supramolecular Chemistry*, Pergamon, New York (1996).
[4] J.M. Lehn. *Angew. Chem. Int. Ed. Engl.*, **29**, 1304 (1990).
[5] J.M. Lehn. *Supramolecular Chemistry*, VCH, Weinheim (1995).
[6] C.N.R. Rao, S. Natarajan, R. Vaidhyanathan. *Angew. Chem. Int. Ed.*, **43**, 1466 (2004).

[7] O.M. Yaghi, M. O'Keeffe, N.W. Ockwig, H.K. Chae, M. Eddaoudi, J. Kim. *Nature*, **423**, 705 (2003).

[8] B.F. Abrahams, A. Hawley, M.G. Haywood, T.A. Hudson, R. Robson, D.A. Slizys. *J. Am. Chem. Soc.*, **126**, 2894 (2004).

[9] B.J. Holliday, C.A. Mirkin. *Angew. Chem. Int. Ed.*, **40**, 2022 (2001).

[10] S.V. Kolotuchin, E.E. Fenlon, S.R. Wilson, C.J. Loweth, S.C. Zimmerman. *Angew. Chem. Int. Ed.*, **34**, 2654 (1995).

[11] (a) C. Streb, D.L. Long, L. Cronin. *Cryst. Eng. Commun.*, **8**, 629 (2006); (b) V. Coué, R. Dessapt, M.B. Doeuff, M. Evain, S. Jobic. *Inorg. Chem.*, **46**, 2824 (2007); (c) H. Kumagai, M. Arishima, S. Kitagawa, K. Ymada, S. Kawata, S. Kaizaki. *Inorg. Chem.*, **41**, 1989 (2002); (d) Z.G. Han, Y.L. Zhao, J. Peng, A.X. Tian, Q. Liu, J.F. Ma, E.B. Wang, N.H. Hu. *Cryst. Eng. Commun.*, **7**, 380 (2005); (e) F.F. Jian, H.L. Xiao, Z.R. Zhao, P.P. Sun, P.S. Zhao. *Inorg. Chem. Commun.*, **7**, 1100 (2004); (f) Y.B. Huang, J.X. Chen, T.Y. Lan, X.Q. Lu, C.X. Wei, Z.S. Li, Z.C. Zhang. *J. Mol. Struct.*, **783**, 168 (2006); (g) M.H. Alizadeh, K.T. Holman, M. Mirzaei, H. Razavi. *Polyhedron*, **25**, 1567 (2006); (h) J.L. Xie. *J. Coord. Chem.*, **61**, 3993 (2008); (i) H.L. Chen, Y. Ding, X.X. Xu, E.B. Wang, W.L. Chen, S. Chang, X.L. Wang. *J. Coord. Chem.*, **62**, 347 (2009); (j) W. Wang, Y. Liu, G.L. Xue, H.M. Hu, F. Fu, J.W. Wang. *J. Coord. Chem.*, **61**, 2499 (2008); (k) M.X. Li, G.L. Guo, J.Y. Niu. *J. Coord. Chem.*, **61**, 2896 (2008).

[12] (a) W.J. Duan, X.B. Cui, Y. Xu, J.Q. Xu, H.H. Yu, Z.H. Yi, J.W. Cui, T.G. Wang. *J. Solid State Chem.*, **180**, 1875 (2007); (b) Z.H. Yi, X.B. Cui, X. Zhang, G.D. Yang, J.Q. Xu, X.Y. Yu, H.H. Yu, W.J. Duan. *J. Mol. Struct.*, **891**, 123 (2008); (c) X.B. Cui, K.C. Li, L. Ye, Y. Chen, J.Q. Xu, W.J. Duan, H.H. Yu, Z.H. Yi, J.W. Cui. *J. Solid State Chem.*, **181**, 221 (2008); (d) S.Y. Shi, Y. Chen, B. Liu, Y.K. Lu, J.N. Xu, X.B. Cui, J.Q. Xu. *J. Coord. Chem.*, **62**, 2937 (2009); (e) J.W. Cui, Y. Chem, X.B. Cui, H.H. Yu, J.N. Xu, J.Q. Xu, W.J. Duan, T.G. Wang. *J. Solid State Chem.*, **182**, 1913 (2009).

[13] X.B. Cui, J.Q. Xu, Y. Li, Y.H. Sun, L. Ye, G.Y. Yang. *J. Mol. Struct.*, **657**, 395 (2003).

[14] (a) H. Zhang, L. Duan, Y. Lan, E. Wang, C. Hu. *Inorg. Chem.*, **42**, 8053 (2003); (b) Y. Lu, Y. Xu, E. Wang, J. Lü, C. Hu, L. Xu. *Cryst. Growth Des.*, **5**, 275 (2005); (c) N. Gharah, K. Chowdhury, M. Mukherjee, R. Bhattacharyya. *Transit. Met. Chem.*, **33**, 635 (2008); (d) X. Kong, Y. Ren, P. Zheng, Y. Long, L. Long, R. Huang, L. Zheng. *Inorg. Chem.*, **45**, 10702 (2006); (e) X. Wang, Y. Guo, Y. Li, E. Wang, C. Hu, N. Hu. *Inorg. Chem.*, **42**, 4135 (2003).

[15] (a) P. Zheng, Y. Ren, L. Lomg, R. Huang, L. Zheng. *Inorg. Chem.*, **44**, 1190 (2005); (b) J.A.F. Gamelas, F.M. Santos, V. Felix, A.M.V. Cavaleiro, E.M. Gomes, M. Belsley, M.G.B. Drew. *Dalton Trans.*, 1197 (2006); (c) C. Ritchie, E.M. Burkholder, D. Long, D. Adam, P. Kögerler, L. Cronin. *Chem. Commun.*, 468 (2007).

[16] Q.H. Wei, L.Y. Zhang, G.Q. Yin, L.X. Shi, Z.N. Chen. *J. Am. Chem. Soc.*, **126**, 9940 (2004).

[17] (a) X.M. Zhang, M.L. Tong, X.M. Chen. *Angew. Chem. Int. Ed.*, **41**, 1029 (2002); (b) Y.H. Sun, J.H. Yu, X.J. Jin, J.F. Song, J.Q. Xu, L. Ye. *Inorg. Chem. Commun.*, **9**, 1087 (2006).

[18] X.M. Zhang, J.J. Hou, H.S. Wu. *Dalton Trans.*, 3437 (2004).

[19] Y. Yan, C.D. Wu, C.Z. Lu. *Z. Anorg. Allg. Chem.*, **629**, 1991 (2003).

[20] (a) R.G. Xiong, X. Xue, H. Zhao, X.Z. You, B.F. Abrahams, Z.L. Xue. *Angew. Chem. Int. Ed.*, **41**, 3800 (2002); (b) X. Xue, X.S. Wang, L.Z. Wang, R.G. Xiong, B.F. Abrahams, X.Z. You, Z.L. Xue, C.M. Che. *Inorg. Chem.*, **41**, 6544 (2002).

[21] J.K. Cheng, Y.G. Yao, J. Zhang, Z.J. Li, Z.W. Cai, X.Y. Zhang, Z.N. Chen, Y.B. Chen, Y. Kang, Y.Y. Qin, Y.H. Wen. *J. Am. Chem. Soc.*, **126**, 7796 (2004).

[22] O.R. Evans, W. Lin. *Acc. Chem. Res.*, **35**, 511 (2002).

[23] D. Li, T. Wu. *Inorg. Chem.*, **44**, 1175 (2005).

[24] X.X. Hu, J.Q. Xu, P. Cheng, X.Y. Chen, X.B. Cui, J.F. Song, G.D. Yang, T.G. Wang. *Inorg. Chem.*, **43**, 2261 (2004).

[25] (a) J.M. Knaust, S.W. Keller. *Inorg. Chem.*, **41**, 5650 (2002); (b) J. Lu, D.Q. Chu, J.H. Yu, X. Zhang, M.H. Bi, J.Q. Xu, X.Y. Yu, Q.F. Yang. *Inorg. Chim. Acta*, **359**, 2495 (2006).

[26] X.M. Zhang. *Coord. Chem. Rev.*, **249**, 1201 (2005).

[27] (a) M.A. Porai-Koshits, V.S. Sergienko, É.N. Yurchenko. *J. Struct. Chem.*, **27**, 176 (1986); (b) V.S. Sergienko, M.A. Porai-Koshits, É.N. Yurchenko. *J. Struct. Chem.*, **25**, 133 (1984); (c) V.S. Sergienko, M.A. Porai-Koshits, É.N. Yurchenko. *J. Struct. Chem.*, **21**, 87 (1980).

[28] M.H. Alizadeh, K.T. Holman, M. Mirzaei, H. Razavi. *Polyhedron*, **25**, 1567 (2006).

[29] S. Lin, Y.Z. Yea, X.F. Zhang, C.L. Liu. *Transit. Met. Chem.*, **31**, 760 (2006).

[30] B. Carlo, B. Matrio, F. Vincezo. *Chem. Mater.*, **8**, 1475 (1995).

[31] L.H. Bi, E.B. Wang, L. Xu, R.D. Huang. *Inorg. Chim. Acta*, **163**, 305 (2000).

[32] D. Altermatt, I.D. Brown. *Acta Crystallogr. B*, **41**, 240 (1985).

[33] N. Gharah, K. Chowdhury, M. Mukherjee, R. Bhattacharyya. *Transit. Met. Chem.*, **33**, 635 (2008).

[34] (a) Y. Gong, C.W. Hu, H. Li, W. Tang, K.L. Huang, W.B. Hou. *J. Mol. Struct.*, **784**, 228 (2006); (b) R. Cao, S.X. Liu, J.F. Cao, L. Wang, Q. Tang, Y. Liu, Y.H. Ren. *J. Mol. Struct.*, **888**, 307 (2008).

[35] R. Thouvenot, M. Fournier, R. Franck, C. Rocchiccioli-Deltcheff. *Inorg. Chem.*, **23**, 598 (1984).

[36] Q.G. Zhai, X.Y. Wu, S.M. Chen, Z.G. Zhao, C.Z. Lu. *Inorg. Chem.*, **46**, 5046 (2007).